Raman optical activity demonstrates poly(L-proline) II helix in the N-terminal region of the ovine prion protein: Implications for function and misfunction

doi:10.1016/j.jmb.2004.08.058 J. Mol. Biol. (2004) 343, 467–476

JMB

Available online at www.sciencedirect.com

SCIENCE DIRECT®

ELSEVIER

Raman Optical Activity Demonstrates Poly(L-proline) II Helix in the N-terminal Region of the Ovine Prion Protein: Implications for Function and Misfunction

Ewan W. Blanch[1], Andrew C. Gill[2]*, Alexandre G. O. Rhie[2], James Hope[2] Lutz Hecht[1], Kurt Nielsen[3] and Laurence D. Barron[1]*

[1]*Department of Chemistry University of Glasgow, Glasgow G12 8QQ, UK*

[2]*Institute for Animal Health Compton, Newbury, Berkshire RG20 7NN, UK*

[3]*Department of Chemistry DTU 207, Technical University of Denmark, DK-2800 Lyngby Denmark*

**Corresponding authors*

The aqueous solution structure of the full-length recombinant ovine prion protein PrP^{25-233}, together with that of the N-terminal truncated version PrP^{94-233}, have been studied using vibrational Raman optical activity (ROA) and ultraviolet circular dichroism (UVCD). A sharp positive band at $\sim 1315\ cm^{-1}$ characteristic of poly(L-proline) II (PPII) helix that is present in the ROA spectrum of the full-length protein is absent from that of the truncated protein, together with bands characteristic of β-turns. Although it is not possible similarly to identify PPII helix in the full-length protein directly from its UVCD spectrum, subtraction of the UVCD spectrum of PrP^{94-233} from that of PrP^{25-233} yields a difference UVCD spectrum also characteristic of PPII structure and very similar to the UVCD spectrum of murine PrP^{25-113}. These results provide confirmation that a major conformational element in the N-terminal region is PPII helix, but in addition show that the PPII structure is interspersed with β-turns and that little PPII structure is present in PrP^{94-233}. A principal component analysis of the ROA data indicates that the α-helix and β-sheet content, located in the structured C-terminal domain, of the full-length and truncated proteins are similar. The flexibility imparted by the high PPII content of the N-terminal domain region may be an essential factor in the function and possibly also the misfunction of prion proteins.

Keywords: ovine prion protein; transmissible spongiform encephalopathy; poly(L-proline) II helix; Raman optical activity; amyloid fibrils

Introduction

Prion proteins are associated with a variety of neurodegenerative diseases, known as transmissible spongiform encephalopathies (TSE), characterised by the presence of spongiform degeneration and astrocytic gliosis.[1] Despite much effort, an understanding of some key aspects of TSE disease remains elusive, such as the existence of an infectious form along with genetic and sporadic forms, something that has not been recognised in any other class of neurodegenerative disease. The basic current model involves conversion of a ubiquitous cellular form of the prion protein (PrP^C) into a scrapie (amyloid fibril) form (PrP^{Sc}), the prion protein being both target and infectious agent. PrP^C has a high proportion of α-helical structure, is soluble in detergents and is susceptible to proteolysis. Conversely, PrP^{Sc} has a high β-sheet content, is insoluble in detergents and is partially resistant to proteolysis. Further understanding of TSE disease requires more detailed knowledge of the solution structures of prion proteins and the conformational changes associated with the possible different transformation pathways of PrP^C into PrP^{Sc} that are involved in the infectious, genetic and sporadic forms.[2]

After expression and post-translational processing, PrP^C has between 208 and 220 amino acid residues depending on mammalian species, two N-glycan linkage sites of variable occupancy and a C-terminal glycosyl-phosphatidylinositol (GPI) membrane anchor. Structural analysis by Fourier

Abbreviations used: PPII, poly(L-proline) II helix; PrP, prion protein; ROA, Raman optical activity; TSE, transmissible spongiform encephalopathy; UVCD, ultraviolet circular dichroism.

E-mail addresses of the corresponding authors: laurence@chem.gla.ac.uk; andrew.gill@bbsrc.ac.uk

transform infrared (FTIR) and ultraviolet circular dichroism (UVCD) spectroscopy indicated that PrP^{C} contains ~40% α-helix and little β-sheet, whilst PrP^{Sc} contains ~30% α-helix and ~45% β-sheet.[3,4] Although there have been numerous NMR studies on the solution structure of PrP^{C},[5] X-ray crystallographic studies have been hampered by difficulties in crystallising the protein. The NMR structures of full-length recombinant prion proteins of different mammalian species all revealed a structured C-terminal globular domain containing mainly α-helical sequences in the form of a compact three-helix bundle, and a long flexibly disordered N-terminal domain of 80–100 amino acid residues, which includes a metal ion binding octapeptide repeat motif.[6] Recently, however, the first crystal structure of a monomeric recombinant prion protein, namely ovine PrP, has been solved[7] and found to be very similar to the solution NMR structures of other mammalian species. For crystallisation, only the folded C-terminal domain 128–233 was present. This structure of ovine $PrP^{128\text{-}233}$ is represented pictorially in Figure 1.

An increasing amount of research is focusing on the contribution of the disordered N-terminal region to PrP^{C} function. Previously, the role of this region in the disease process tended to be overlooked mainly because a long N-terminal segment of PrP^{Sc} is lost on *in vitro* proteolytic digestion of PrP^{Sc} to the core structure PrP27-30 (meaning a protein of between 27 kDa and 30 kDa). In addition, transgenic mice that are devoid of much of the N-terminal region still support prion replication,[8,9] indicating that the N-terminal region is not required *a priori* for the conversion process. However, immunologic studies of PrP^{Sc} suggest that the conformational change that occurs during conversion of PrP^{C} into PrP^{Sc} is mostly in the region from residues ~94–149 or perhaps 179 with the major changes localised largely to a part of the disordered N-terminal region bounded by residues ~94 and ~124,[10,11] and Donne *et al.*[12] have suggested that the N-terminal region could feature in the conversion of PrP^{C} to PrP^{Sc} by template-assisted formation of β-structure. Furthermore, recent evidence suggests that the presence of the N-terminal region could play a key role in determining the conformation of PrP^{Sc} and in modulating cross-species disease transmission and TSE pathogenesis.[13] Thus, the impact of the N-terminal region on the structure of mature length PrP is clearly of considerable importance in TSE disease.

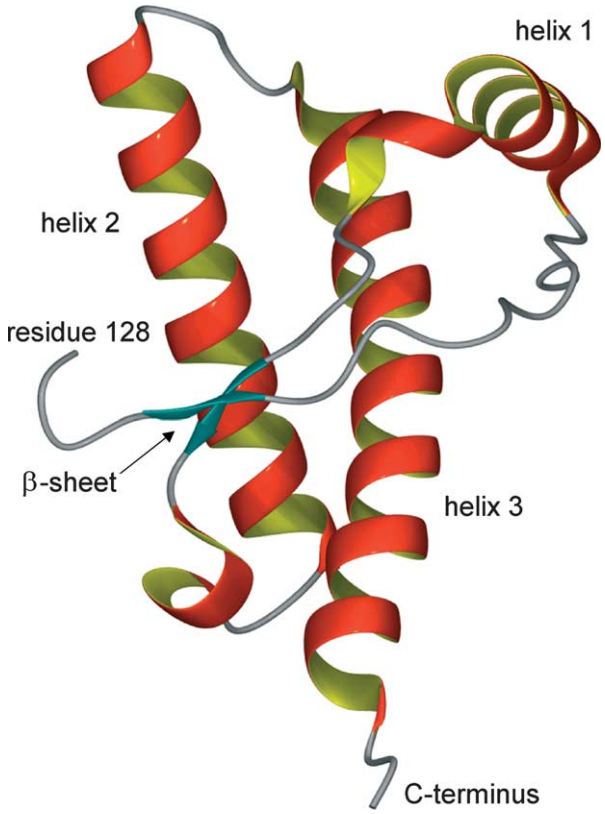

Figure 1. The tertiary structure of the globular, C-terminal domain of the ovine prion protein as determined by X-ray crystallography.[7] The structure was rendered using Molmol and Povray.

Many reports of structural characterisation of the octapeptide repeat region of the N-terminal domain of PrP^{Sc} complexed with copper ions exist, including a recent crystal structure of copper complexed to a pentapeptide derived from the prion N terminus.[14] Conversely, there is scant information on the structure of this domain in isolation, primarily because the detailed characterisation of non-regular peptide sequences in proteins is difficult using standard solution phase structural techniques such as NMR and UVCD. However, it has recently been shown that Raman optical activity (ROA), which measures vibrational optical activity by means of a small difference in the intensity of Raman scattering from chiral molecules in right- and left-circularly polarised incident laser light,[15–18] is able to provide new information about the structure of disordered sequences in intact proteins in aqueous solution.[19] This work suggests that an important conformational element in such sequences is poly(L-proline) II (PPII) helix. Although originally defined for the conformation adopted by polymers of L-proline, PPII helix can be supported by amino acid sequences other than those based on L-proline and has been recognised as a common structural motif within loops in the X-ray crystal structures of many proteins.[20] It consists of a left-handed helix with 3-fold rotational symmetry in which the ϕ, ψ angles of the constituent residues have values around $-78°$, $+146°$, corresponding to a region of the Ramachandran surface to one side of the β-region. The extended nature of the PPII helix precludes intrachain hydrogen bonds, the structure being stabilised instead by main-chain hydrogen bonding with water molecules and side-chains.[21]

PPII helix currently attracts much interest as a major conformational element of disordered polypeptides and unfolded proteins in aqueous solution.[22] PPII structure can be distinguished from random coil in polypeptides by UVCD,[22,23]

vibrational circular dichroism (VCD),[24] FTIR and Raman[25] and ultraviolet Raman,[26] but these techniques are less sensitive than ROA to PPII structure when there are a number of other conformational elements present as in proteins. Although the lack of main-chain hydrogen bonding makes NMR determinations of PPII structure difficult, a recent NMR study, complemented by UVCD, of a peptide sequence containing seven alanine residues provides strong evidence for a predominantly PPII conformation in aqueous solution.[27] A subsequent ROA study of a similar peptide firmly demonstrated the ability of ROA to identify PPII structure.[28] PPII helix may be important in the regulatory multiple weak interactions that are increasingly being recognised as associated with intrinsically unstructured peptide sequences within proteins.[23,29–32] Furthermore, proteins that are completely unfolded in their native state may contain a large amount of PPII helix, which imparts a rheomorphic (flowing shape) character to their structure[33] and which appears to be important for their function.[34]

The presence of significant amounts of PPII structure in the N-terminal disordered region of the prion protein has already been suggested from UVCD studies of synthetic polypeptides based on the octarepeat region.[35,36] Subsequent UVCD studies of the N-terminal peptide $PrP^{40\text{-}57}$ showed that it can also form a PPII structure in aqueous buffer, with the discovery of 4-hydroxyproline in recombinant PrP from Chinese hamster ovary cells and PrP^{Sc} from terminally infected mouse brains providing proof for the formation of PPII helix in PrP *in vivo*.[37] In addition, NMR measurements of peptides derived from the octarepeat region of PrP suggested that certain residues adopt loop and β-turn structures.[38,39]

Here, we report an ROA study of the aqueous solution structures, especially the characterisation of PPII helix, of recombinant ovine prion protein residues 25–233, the sequence of which is given in Figure 2, and the N-terminal truncated protein comprising residues 94–233, in order to obtain new information about the fold of these biomolecules. This information is compared with that derived from UVCD spectra of the same proteins and a C-terminally truncated construct.

```
  1  MVKSH IGSWI LVLFV AMWSD VGLCK KRPKP  30
 31  GGGWN TGGSR YPGQG SPGGN RYPPQ GGGGW  60
 61  GQPHG GGWGQ PHGGG WGQPH GGGWG QPHGG  90
 91  GGWGQ GGSHS QWNKP SKPKT NMKHV AGAAA 120
121  AGAVV GGLGG YMLGS AMSRP LIHFG NDYED 150
151  RYYRE NMYRY PNQVY YRPVD RYSNQ NNFVH 180
181  DCVNI TVKQH TVTTT TKGEN FTETD IKIME 210
211  RVVEQ MCITQ YQRES QAYYQ RGASV ILFSS 240
241  PPVIL LISFL IFLIV G                 256
```

Figure 2. The amino acid sequence of the ovine prion protein. The initial 24 amino acid residues and final 23 amino acid residues comprise the N-terminal and C-terminal signal peptides, respectively. The full-length prion protein starts at lysine 25 (in bold); the N-terminally truncated protein starts at glycine 94 (bold and italic). Both constructs end at the mature C terminus, alanine 233.

Results and Discussion

Figure 3 shows the back-scattered Raman and ROA spectra of ovine $PrP^{25\text{-}233}$ and $PrP^{94\text{-}233}$ in aqueous solution. Despite the high backgrounds to the parent Raman spectra of the two samples, ROA spectra of reasonable quality were obtained by summing the spectra acquired in several different measurement runs. An account of most of the ROA assignments given in what follows can be found.[19,40,41]

PPII helix

A prominent feature in the ROA spectrum of $PrP^{25\text{-}233}$ (Figure 3, top) is the narrow positive band observed at $\sim$1315 cm^{-1} within the extended amide III region ($\sim$1230–1350 cm^{-1}) where normal vibrational modes made up of various combinations of the in-plane N–H deformation (in-phase), the C–N stretch and $C^{\alpha}-H$ deformations

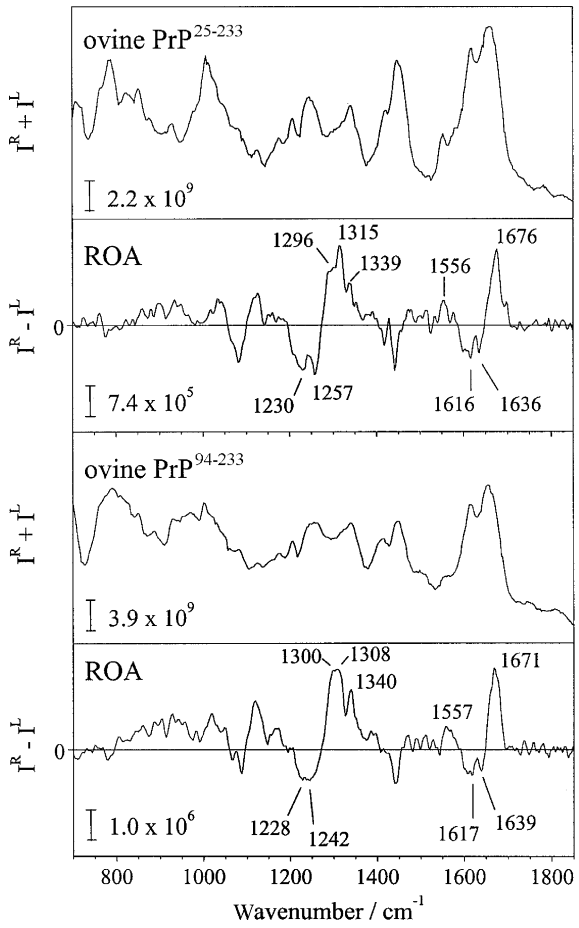

Figure 3. Back-scattered Raman (I^R+I^L) and ROA (I^R-I^L) spectra in sodium acetate buffer (pH 5.5), of ovine $PrP^{25\text{-}233}$ (top pair) and $PrP^{94\text{-}233}$ (bottom pair). The high fluorescence backgrounds have been subtracted from the Raman spectra.

occur. A similar positive band at ~1319 cm^{-1} dominates the ROA spectra of disordered poly (L-lysine) and poly(L-glutamic acid).[19] Since these disordered polypeptides are thought to contain substantial amounts of the PPII-helical conformation, perhaps in the form of short segments interspersed with residues having other conformations,[22] this ROA band has been assigned to a vibrational mode of the PPII helix. Similar positive bands are seen in this region in the ROA spectra of some β-sheet proteins where they have been assigned to PPII-helical elements.[16,19] This assignment has been reinforced recently by an ROA study of the aqueous solution structures of a series of alanine oligopeptides, including AcOOAAAAAAAAOO-NH_2, the ROA spectrum of which is dominated by a positive ROA band at ~1319 cm^{-1}.[28] This peptide is similar to the one shown by Shi *et al*.[27] to adopt a predominantly PPII conformation. $PrP^{25\text{-}233}$ therefore appears to contain a significant number of residues in the PPII conformation. Since the positive ~1315 cm^{-1} band is absent from the ROA spectrum of $PrP^{94\text{-}233}$ (Figure 3, bottom), we deduce that most of the PPII sequences are located in the N-terminal 23–89 fragment. Also missing from the $PrP^{94\text{-}233}$ ROA spectrum are the negative and positive bands at ~1257 cm^{-1} and 1296 cm^{-1}, respectively, assigned to β-turns,[40] from which we deduce that the 23–89 fragment also contains β-turns. These results are consistent with the previous suggestions of both PPII and β-turns in the N-terminal region.[35–39]

The UVCD spectra of ovine $PrP^{25\text{-}233}$ and $PrP^{94\text{-}233}$ are displayed in Figure 4(a). Both show characteristic minima at ~222 nm and 208 nm, indicating a predominance of α-helix in the structures. Although the UVCD spectra are qualitatively very similar, they are quantitatively different. These differences arise either from differences in the folded domains of each protein or from the presence of the N-terminal region in $PrP^{25\text{-}233}$. Since NMR determinations of PrP globular structures indicated only subtle differences in these regions when the N-terminal region was incorporated, we believe that the differences in the UVCD spectra reflect the contributions made to the spectra by the N-terminal region.

Subtraction of the UVCD spectrum of $PrP^{94\text{-}233}$ from that of $PrP^{25\text{-}233}$ yields a difference spectrum (Figure 4(b)) with a strong negative minimum at ~195 nm and a weak positive maximum at ~220–230 nm characteristic of PPII-helix,[22,23] which, in agreement with the conclusions from the ROA data, may be ascribed to PPII structure in the 25–93 fragment. This spectrum is similar to those previously determined for the octapeptide repeat region[35,36] and for a peptide spanning residues 40–57.[37] To further confirm the similarities between these spectra, in Figure 4(b) we also present the UVCD spectrum of a polypeptide derived from murine PrP spanning residues 25–113, which is very similar to the subtracted spectrum and to previous spectra of N-terminal sequences. It also has a maximum at 220–230 nm and a minimum at ~200 nm characteristic of PPII helix. Unfortunately, this polypeptide was only sparingly soluble in physiological buffers and was therefore not amenable to ROA analysis.

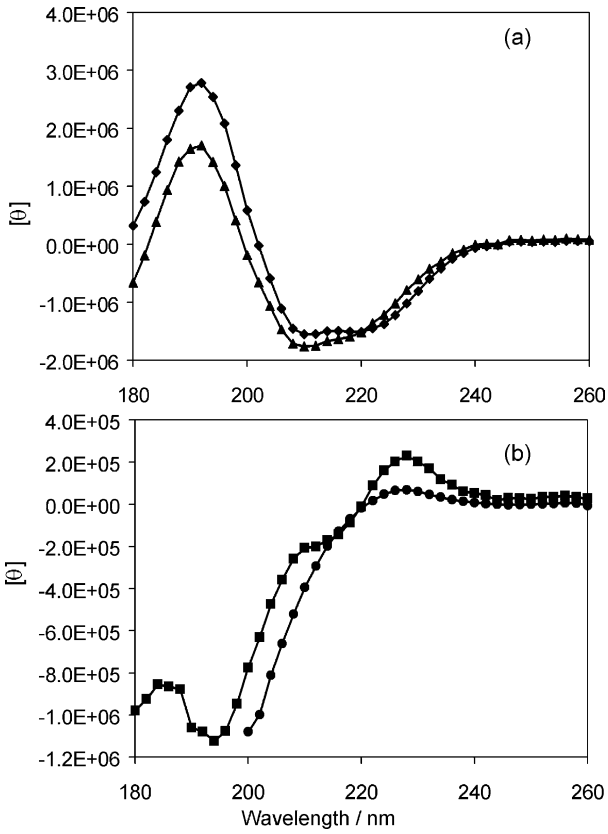

Figure 4. (a) UVCD spectra of recombinant ovine $PrP^{25\text{-}233}$ (triangles) and $PrP^{94\text{-}233}$ (diamonds). (b) Subtracted UVCD spectrum of $PrP^{25\text{-}233}$–$PrP^{94\text{-}233}$ (squares) together with the UVCD spectrum of murine $PrP^{25\text{-}113}$ (circles). The units of the molar ellipticity [θ] are degrees cm^2/mol.

α-Helix and β-sheet: principal component analysis

Useful ROA signatures of α-helix include positive extended amide III bands at ~1300–1310 cm^{-1} and ~1340 cm^{-1} characteristic of unhydrated and hydrated versions, respectively, and an amide I couplet centred at ~1650 cm^{-1} that is negative at low wave number and positive at high.[41] Useful β-sheet ROA signatures include negative bands at ~1220 cm^{-1} and 1245 cm^{-1} possibly associated with hydrated and unhydrated variants, respectively, and a similar amide I ROA couplet to that generated by α-helix but shifted by ~10 cm^{-1} to higher wave number.[40]

We are developing a pattern recognition program, based on principal component analysis (PCA), to identify protein structural types from ROA band patterns.[40] From the ROA spectral data,

PCA calculates a set of sub-spectra that serve as basis functions, the algebraic combination of which with appropriate expansion coefficients can be used to reconstruct any member of the original set of experimental ROA spectra. Figure 5 shows a plot of the coefficients for our current set of 80 polypeptide, protein and virus ROA spectra for the two most important basis functions. This map provides a two-dimensional representation of the structural relationships among the members of the set. The protein positions are colour-coded with respect to the seven different structural types listed in the Figure and which provide a useful initial classification that will be refined in later work to give quantitative estimates of structural elements such as helix, sheet, loops and turns. The spectra separate into clusters corresponding to different dominant types of protein structural elements, with increasing α-helix content to the left, increasing β-sheet content to the right, and increasing disordered or irregular structure from bottom to top. $PrP^{25\text{-}233}$ and $PrP^{94\text{-}233}$ lie close together near the centre of the alpha beta region, which reinforces the impression from visual inspection of their ROA spectra of a significant amount of β-structure in both in addition to the expected α-helix. This also suggests little difference in the amounts of α-helix and β-sheet in the full-length and truncated proteins. However, $PrP^{94\text{-}233}$ lies below $PrP^{25\text{-}233}$, consistent with the absence of the disordered N-terminal region. Disordered poly(L-lysine), poly(L-glutamic acid) and the $AcOOAAAAAAAOO\text{-}NH_2$ peptide lie towards the top of the Figure.

The similar amount of α-helix in $PrP^{25\text{-}233}$ and $PrP^{94\text{-}233}$ revealed by ROA is consistent with the NMR solution structures, which indicate almost identical amounts of α-helix in full-length and truncated prion proteins (for example, PDB structures 1qlz and 1qml for the resolved sequence 128–231 in human $PrP^{25\text{-}233}$ and $PrP^{94\text{-}233}$ contain 51.9% and 51.0% α-helix, respectively). However, our ROA data reflect a higher β-sheet content than that expected from the solution NMR structures (~3–9% in sequence 125–228). This may be due to oligomerisation at the high concentrations of ovine $PrP^{25\text{-}233}$ and $PrP^{94\text{-}233}$ used (~40 mg/ml). Analytical ultracentrifugation showed our samples to be monomeric at ~5 mg/ml (data not shown) but we anticipate the formation of dimers and oligomers at higher concentrations.

On the basis of recent work on model β-sheet polypeptides and proteins,[40] the positive ROA band at ~1557 cm^{-1} (amide II) and negative ROA band at ~1616 cm^{-1} (amide I) in the spectra of $PrP^{25\text{-}233}$ and $PrP^{94\text{-}233}$ suggest the presence of multi-stranded β-sheet that is more flat and uniform than that found in typical β-sheet proteins. Again this may reflect some oligomerisation.

Implications for prion function and aggregation

Sequence analysis revealed that the N-terminal region of PrP^{C} is highly conserved between species,[42,43] which suggests that it has an important

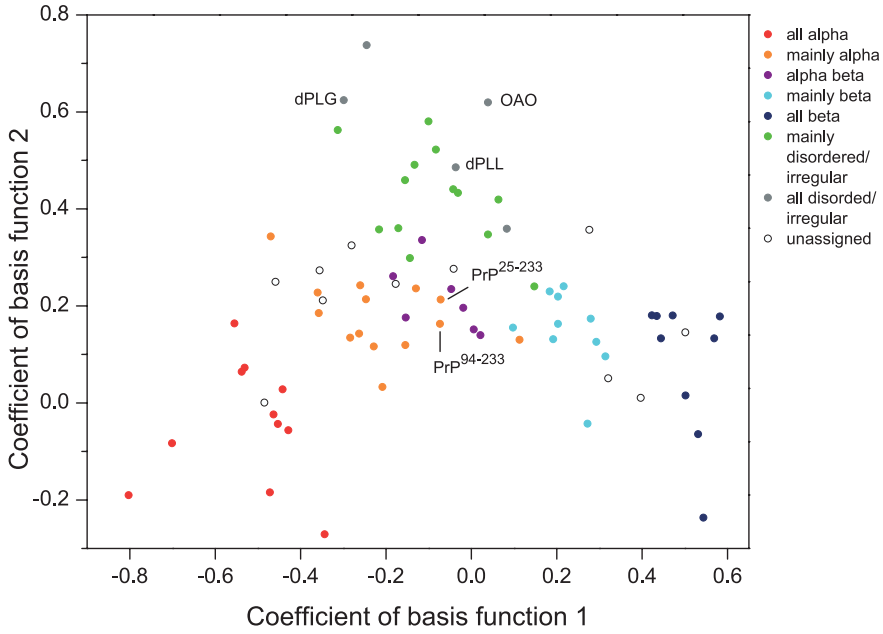

Figure 5. Plot of the PCA coefficients for the two most important basis functions for a set of 80 polypeptide, protein and virus ROA spectra. More complete definitions of the structural types are: all alpha, > ~60% α-helix with little or no other secondary structure; mainly alpha, > ~35% α-helix and a small amount of β-sheet (~5–15%); alpha beta, similar significant amounts of α-helix and β-sheet; mainly beta, > ~35% β-sheet and a small amount of α-helix (~5–15%); all beta, > ~45% β-sheet with little or no other secondary structure; mainly disordered/irregular, little secondary structure; all disordered/irregular, no secondary structure. dPLL, dPLG and OAO denote disordered poly(L-lysine), disordered poly(L-glutamic acid) and $AcOOAAAAAAAOO\text{-}NH_2$, respectively.

structural and functional role.[44] The results of some studies indicate that this functional role involves copper metabolism:[6] four Cu^{2+} ions bind to the protein in the highly conserved group of octapeptide repeats, having the consensus sequence PHGGGWGQ and spanning residues 54–95 in the ovine prion protein, with a fifth taken up in the flexible region between the octarepeats and the globular C-terminal region.[45] Presumably the rheomorphic character of the PPII-rich N-terminal region of the apoprotein, together with the ability of the four glycine residues within each octarepeat to support turns and extended structure as well as PPII, enables the appropriate sequences to readily adapt to the fixed Cu(II)-bound conformation of the holoprotein. This conformational adaptability may also be important in binding of PrP to other ligands within the intra- or extra-cellular environments. Various binding partners for the N-terminal region of PrP have been suggested, including polyanions,[46] the laminin receptor[47] and nucleic acids.[48] It is therefore likely that an extended, rather flexible structure in this region is important in promoting binding and facilitating molecular interactions.

An ROA study revealed that PPII helix is formed at the expense of hydrated α-helix in the prefibrillar amyloidogenic intermediate of human lysozyme, which prompted the suggestion that PPII helix could be a critical conformational element in some amyloid diseases.[49] Elimination of water molecules between extended PPII chains having hydrated backbone C═O and N–H groups to form β-sheet hydrogen bonds is a favourable thermodynamic process.[50] Since PPII chains are close in conformation to β-strands, they would be expected to readily undergo this type of aggregation with each other and with established β-sheet. A more recent study using conventional techniques has corroborated this idea, but without explicitly identifying the extended polypeptide chains as PPII-type structure.[51] A subsequent ROA study of the brain proteins α-synuclein and tau, which have a propensity to form the fibrils associated with Parkinson's and Alzheimer's disease, respectively, revealed that these natively unfolded proteins consist largely of PPII helical sequences.[33] However, although disorder of the PPII type may be essential for the formation of regular fibrils, the presence of a large amount of PPII structure does not necessarily impart a fibrillogenic character since not all PPII-rich non-regular protein structures form amyloid fibrils. For example, the casein milk proteins and the brain proteins β- and γ-synuclein show little propensity for amyloid fibril formation and are not associated with disease, yet their natively unfolded structures are based largely on PPII sequences as in α-synuclein, which is highly amyloidogenic.[33] A more complete understanding of the fibrillogenic propensity of a particular sequence, PPII or otherwise, requires knowledge of the various physicochemical properties of the constituent residues.[52] In particular, a combination of high net charge and low mean hydrophobicity has been shown to be an important prerequisite for protein sequences to remain natively unfolded.[34,53]

The potential importance of PPII in amyloid disease has been reinforced by recent demonstrations of the presence of significant amounts of this conformation in the Alzheimer amyloid peptide Aβ(12–28) by UVCD[54] and in Aβ(1–28) by FTIR and Raman.[55] The latter study also identified the presence of β-strand.

There have been some recent attempts to use spectroscopic data to quantify the propensities of different residues to adopt the PPII conformation.[31,56–58] The 25–93 sequence of the disordered N-terminal region of PrP^C has a high proportion of proline (ten) and glycine (31) residues, many of which occur in the metal-binding group of octarepeats. It appears that glycine is quite favourable for PPII formation, perhaps due to backbone solvation,[56] so that, together with the very high PPII propensity of proline itself, the 25–93 sequence is expected to have a high average PPII propensity.

The physicochemical properties of the constituent residues of the disordered N-terminal region are highly relevant to the prion problem. Since PrP^{Sc} formation, and prion propagation, are possible with deletions in PrP^C up to residue ~110, these residues are evidently not playing a critical role in PrP misfolding. In addition, since the protease-resistant core structure of PrP^{Sc} formed from full-length PrP^C contains only residues ~90–233, most of the N-terminal sequence appears not to participate in the compact folded domain of PrP^{Sc}. It therefore appears that, despite the high PPII content revealed by the present study, the 25–93 sequence of the disordered N-terminal region of PrP^C is not intrinsically fibrillogenic. Due to the presence of four positively charged residues in the extreme N-terminal sequence KKRPKP, the N-terminal end carries a high net charge and also has a low mean hydrophobicity. Although the mean hydrophobicity of the rest of the 25–93 sequence is only average, ~59% of the sequence is made up of proline and glycine residues, which have very low β-sheet forming propensities.[59] The 25–93 sequence of the disordered N-terminal region therefore appears to be well protected against association into β-sheet structures.

Comparison of the solution NMR structures of full-length and truncated prion proteins revealed that the N-terminal region has a small but significant stabilising influence on certain sequences of the structured C-terminal domain. The first indication of this was the detection of a stabilisation of helical structure associated with residues 190–196 within helix 2 of the hamster prion protein that was suggested to arise from transient tertiary interactions between the N-terminal residues and helix 2 residues.[12] Subsequent studies of human prion protein revealed a similar stabilisation of this segment of helix 2, but also revealed some stabilisation in residues 222–229[60] and 219–225[61] within helix 3, with similar observations for the bovine prion protein.[62] However, the implied

increase of helix population amounts only to a few percent,[60] as confirmed by our ROA results. So although not directly participating in the β-fibril formation responsible for prion disease, it appears from these NMR studies that there is scope for the disordered N-terminal region to modulate the fibrillogenesis itself, together with the infectivity and species barriers that characterise prion disease. Certainly, this was born out in recent investigations of cross-species disease transmission *in vivo* and *in vitro*.[13]

Conclusions

ROA has revealed that a major conformational element in the "disordered" N-terminal region of the full-length ovine prion protein $PrP^{25\text{-}233}$ is PPII helix, which was confirmed by UVCD, and that some β-turns are also present. ROA further revealed that little PPII structure is present in the truncated protein $PrP^{94\text{-}233}$ and that the amounts of α-helix in the full-length and truncated proteins are very similar. The presence of a large amount of PPII structure in the N-terminal region is consistent with the flexibility required for its ability to bind metal ions and for its apparent ability to modulate properties of the full-length protein *via* interactions with the structured C-terminal region. Changes in environmental factors, or of the physicochemical properties of critical residues associated with genetic variants, could readily modify subtle characteristics such as fibrillogenic propensity of particular sequences within the N-terminal region itself or within regions of the C-terminal domain that interact with this region. Hence, the PPII-rich character of the N-terminal region appears to be an essential factor in the function, and possibly a modulating factor in the misfunction, of prion proteins.

Materials and Methods

Materials

Recombinant prion proteins were produced as described.[63,64] Briefly, PrP proteins were expressed from the pTrc plasmid (Quiagen) either without (PrP25-233) or with (PrP94-233) the hexHis tag in *Escherichia coli* cells. Protein production was induced by the addition of IPTG and cells were harvested by centrifugation. Cells were lysed using lysozyme and inclusion bodies harvested by centrifugation after removal of DNA by treatment with sodium deoxycholate and DNase. Protein from inclusion bodies was solubilised in 8 M urea and PrP purifed by immobilised metal ion affinity chromatography followed by cation exchange chromatography. The single disulphide bond was remade by incubation with fivefold molar excess of copper ions followed by extensive dialysis against 50 mM sodium acetate to refold the protein. Final fractions were checked by SDS-PAGE, UVCD and electrospray mass spectrometry (ESMS). Concentrations were determined by UV absorbance.

To produce fractions of sufficient concentration for ROA spectroscopy, protein was concentrated in filtration concentration devices of progressively smaller size (centriprep, centricon, microcon; Amicon). Final concentration was done by removal of solvent under vacuum. The fidelity of the protein was checked after concentration by removal of a 1 μl aliquot, dilution and analysis by UVCD and ESMS.

DNA encoding the murine PrP sequence 25–113 was cloned from a template of the full-length protein and inserted into the pTrc expression plasmid (Quiagen). Transformed *E. coli* were used for expression of the protein, which was isolated as described above. Yields of this polypeptide were poor and the final fraction was only sparingly soluble in 50 mM sodium acetate (pH 5.5).

ROA spectroscopy

The instrument used for the Raman and ROA measurements has a back-scattering configuration, which is essential for ROA studies of aqueous solutions of biopolymers, and employs a single-grating spectrograph fitted with a back-thinned CCD camera as detector and an edge filter to block the Rayleigh line.[65] ROA is measured by synchronising the Raman spectral acquisition with an electro-optic modulator to switch the polarisation state of the incident argon-ion laser beam between right and left circular at a suitable rate. The spectra are displayed in analog-to-digital counter units as a function of the Stokes wave number shift with respect to the exciting laser wave number. The ROA spectra are presented as circular intensity differences $I^R - I^L$ and the parent Raman spectra as circular intensity sums $I^R + I^L$, where I^R and I^L are the Raman-scattered intensities in right- and left-circularly polarised incident light, respectively.

The $PrP^{25\text{-}233}$ and $PrP^{94\text{-}233}$ solutions were studied at concentrations ~40 mg/ml in ~50 mM acetate buffer (pH 5.5), at ambient temperature (~20 °C). The solutions were filtered through 0.22 μm Millipore filters into quartz microfluorescence cells, which were centrifuged gently prior to mounting in the ROA instrument. Residual visible fluorescence from traces of impurities, which can give large backgrounds in Raman spectra, was quenched by leaving the samples to equilibrate in the laser beam for a few hours before acquiring ROA data. The experimental conditions were as follows: laser wavelength, 514.5 nm; laser power at the sample, ~700 mW; spectral resolution, ~10 cm^{-1}; acquisition time, ~50 hours in total for the prion proteins.

UVCD spectroscopy

The UVCD spectra were recorded by use of a Jasco J-710 spectropolarimeter. All samples were dissolved in sodium acetate buffer (pH 5.5). Spectra of $PrP^{25\text{-}233}$ (0.62 mg/ml) and $PrP^{94\text{-}233}$ (0.64 mg/ml) were recorded in a cell of path length 0.01 cm. The spectrum of murine $PrP^{23\text{-}109}$ (0.03 mg/ml) was recorded in a cell of path length 0.2 cm. The spectra were averaged over three individual spectra, each being the sum of at least 20 scans. Concentrations were determined by UV absorbance at 280 nm by use of a Beckman DU650 spectrophotometer.

Acknowledgements

L.D.B. and L.H. thank BBSRC and EPSRC for Research Grants. A.C.G., A.G.O.R. and J.H. thank

BBSRC for funding, I. D. Sylvester and S. M. Whyte for original preparation of recombinant bacteria and M. A. Ritchie for initial help and discussions.

References

1. Prusiner, S. B. (1998). Prions. *Proc. Natl Acad. Sci. USA*, **95**, 13363–13383.
2. Cohen, F. E. & Prusiner, S. B. (1998). Pathologic conformations of prion proteins. *Annu. Rev. Biochem.* **67**, 793–819.
3. Pan, K. M., Baldwin, M., Nguyen, J., Gasset, M., Serban, A., Groth, D. *et al*. (1993). Conversion of α-helices into β-sheets features in the formation of the scrapie prion proteins. *Proc. Natl Acad. Sci. USA*, **90**, 10962–10966.
4. Pergamini, P., Jaffe, H. & Safar, J. (1996). Semipreparative chromatographic method to purify the normal cellular isoform of the prion protein in nondenatured form. *Anal. Biochem.* **236**, 63–73.
5. Wüthrich, K. & Riek, R. (2001). Three-dimensional structures of prion proteins. *Advan. Protein Chem.* **57**, 55–82.
6. Viles, J. H., Cohen, F. E., Prusiner, S. B., Goodin, D. B., Wright, P. E. & Dyson, H. J. (1999). Copper binding to the prion protein: structural implications of four identical cooperative binding sites. *Proc. Natl Acad. Sci. USA*, **96**, 2042–2047.
7. Haire, L. F., Whyte, S. M., Vasisht, N., Gill, A. C., Verma, C., Dodson, E. J. *et al*. (2004). The crystal structure of the globular domain of sheep prion protein. *J. Mol. Biol.* **336**, 1175–1183.
8. Fischer, M., Rulicke, T., Raeber, A., Sailer, A., Moser, M., Oesch, B. *et al*. (1996). Prion protein (PrP) with amino-proximal deletions restoring susceptibility of PrP knockout mice to scrapie. *EMBO J.* **15**, 1255–1264.
9. Supattapone, S., Bosque, P., Muramoto, T., Wille, H., Aagaard, C., Peretz, D. *et al*. (1999). Prion protein of 106 residues creates an artificial transmission barrier for prion replication in transgenic mice. *Cell*, **96**, 869–878.
10. Peretz, D., Williamson, R. A., Matsunaga, Y., Serban, H., Pinilla, C., Bastidas, R. B. *et al*. (1997). A conformational transition at the N terminus of the prion protein features in formation of the scrapie isoform. *J. Mol. Biol.* **273**, 614–622.
11. Korth, C., Stierli, B., Streit, P., Moser, M., Schaller, O., Fischer, R. *et al*. (1997). Prion (PrP^{Sc})-specific epitope defined by a monoclonal antibody. *Nature*, **389**, 74–77.
12. Donne, D. G., Viles, J. H., Groth, D., Mehlhorn, I., James, T. L., Cohen, F. E. *et al*. (1997). Structure of the recombinant full-length hamster prion protein PrP(29-231): the N terminus is highly flexible. *Proc. Natl Acad. Sci. USA*, **94**, 13452–13457.
13. Lawson, V. A., Priola, S. A., Meade-White, K., Lawson, M. & Chesebro, B. (2004). Flexible N-terminal region of prion protein influences conformation of protease resistant prion protein isoforms associated with cross-species scrapie infection *in vivo* and *in vitro*. *J. Biol. Chem.* **279**, 13689–13695.
14. Burns, C. S., Aronoff-Spencer, E., Dunham, C. M., Lario, P., Avdievich, N. I., Antholine, W. E. *et al*. (2002). Molecular features of the copper binding sites in the octarepeat domain of the prion protein. *Biochemistry*, **41**, 3991–4001.
15. Barron, L. D., Bogaard, M. P. & Buckingham, A. D. (1973). Raman scattering of circularly polarized light by optically active molecules. *J. Am. Chem. Soc.* **95**, 603–605.
16. Barron, L. D., Hecht, L., Blanch, E. W. & Bell, A. F. (2000). Solution structure and dynamics of biomolecules from Raman optical activity. *Prog. Biophys. Mol. Biol.* **73**, 1–49.
17. Barron, L. D., Hecht, L., Blanch, E. W. & McColl, I. H. (2002). Raman optical activity comes of age. *Mol. Phys.* **102**, 731–744.
18. Hug, W. (2002). Raman optical activity. In *Handbook of Vibrational Spectroscopy* (Chalmers, J. M. & Griffiths, P. R., eds), vol. 1, pp. 745–758, Wiley, Chichester.
19. Barron, L. D., Blanch, E. W. & Hecht, L. (2002). Unfolded proteins studied by Raman optical activity. *Advan. Protein Chem.* **62**, 51–90.
20. Adzhubei, A. A. & Sternberg, M. J. E. (1994). Conservation of polyproline II helices in homologous proteins: implications for structure prediction by model building. *Protein Sci.* **3**, 2395–2410.
21. Creamer, T. P. & Campbell, M. N. (2002). Determinants of the polyproline II helix from modelling studies. *Advan. Protein Chem.* **62**, 263–282.
22. Shi, Z., Woody, R. W. & Kallenbach, N. (2002). Is polyproline II a major backbone conformation in unfolded proteins? *Advan. Protein Chem.* **62**, 163–240.
23. Bochicchio, B. & Tamburro, A. M. (2002). Polyproline II structure in proteins: identification by chiroptical spectroscopies, stability and functions. *Chirality*, **14**, 782–792.
24. Keiderling, T. A. (2000). Peptide and protein conformational studies with vibrational circular dichroism and related spectroscopies. In *Circular Dichroism. Principles and Applications* (Berova, N., Nakanishi, K. & Woody, R. W., eds), pp. 621–666, Wiley, New York.
25. Schweitzer-Stenner, R., Eker, F., Griebenow, K., Cao, X. & Nafie, L. A. (2004). The conformation of tetraalanine in water determined by polarized Raman, FT-IR and VCD spectroscopy. *J. Am. Chem. Soc.* **126**, 2768–2776.
26. Asher, S. A., Mikhonin, A. V. & Bykov, S. (2004). UV Raman demonstrates that α-helical polyalanine peptides melt to polyproline II conformations. *J. Am. Chem. Soc.* **126**, 8433–8440.
27. Shi, Z., Olson, C. A., Rose, G. D., Baldwin, R. L. & Kallenbach, N. R. (2002). Polyproline II structure in a sequence of seven alanine residues. *Proc. Natl Acad. Sci. USA*, **99**, 9190–9195.
28. McColl, I. H., Blanch, E. W., Hecht, L., Kallenbach, N. R. & Barron, L. D. (2004). Vibrational Raman optical activity characterization of poly(L-proline) II helix in alanine oligopeptides. *J. Am. Chem. Soc.* **126**, 5076–5077.
29. Siligardi, G. & Drake, A. F. (1995). The importance of extended conformations and, in particular, the P_{II} conformation for the molecular recognition of peptides. *Biopolymers*, **37**, 281–292.
30. Wright, P. E. & Dyson, H. J. (1999). Intrinsically unstructured proteins: re-assessing the protein structure–function paradigm. *J. Mol. Biol.* **293**, 321–331.
31. Kelly, M. A., Chellgren, B. W., Rucker, A. L., Troutman, J. M., Fried, M. G., Miller, A. F. &

Creamer, T. P. (2001). Host–guest study of left-handed polyproline II helix formation. *Biochemistry*, **40**, 14376–14383.
32. Dunker, A. K., Brown, C. J., Lawson, J. D., Iakoucheva, L. M. & Obradovic, Z. (2002). Intrinsic disorder and protein function. *Biochemistry*, **41**, 6573–6582.
33. Syme, C. D., Blanch, E. W., Holt, C., Jakes, R., Goedert, M., Hecht, L. & Barron, L. D. (2002). A Raman optical activity study of rheomorphism in caseins, synucleins and tau. New insight into the structure and behaviour of natively unfolded proteins.. *Eur. J. Biochem.* **269**, 148–156.
34. Uversky, V. N. (2003). A protein-chameleon: conformational plasticity of α-synuclein, a disordered protein involved in neurodegenerative disorders. *J. Biomol. Struct. Dyn.* **21**, 211–234.
35. Smith, C. J., Drake, A. F., Banfield, B. A., Bloomberg, G. B., Palmer, M. S., Clarke, A. R. & Collinge, J. (1997). Conformational properties of the prion octa-repeat and hydrophobic sequences. *FEBS Letters*, **405**, 378–384.
36. Whittal, R. M., Ball, H. L., Cohen, F. E., Burlingame, A. L., Prusiner, S. B. & Baldwin, M. A. (2000). Copper binding to octarepeat peptides of the prion protein monitored by mass spectrometry. *Protein Sci.* **9**, 332–343.
37. Gill, A. C., Ritchie, M. A., Hunt, L. G., Steane, S. E., Davies, K. G., Bocking, S. P. *et al*. (2000). Post-translational hydroxylation at the N-terminus of the prion protein reveals presence of PPII structure *in vivo*. *EMBO J.* **19**, 5324–5331.
38. Yoshida, H., Matsushima, N., Kumaki, Y., Nakata, M. & Hikichi, K. (2000). NMR studies of model peptides of PHGGGWGQ repeats within the N-terminus of prion proteins: a loop conformation with histidine and tryptophan in close proximity. *J. Biochem.* **128**, 271–281.
39. Zahn, R. (2000). The octapeptide repeats in mammalian prion protein constitute a pH-dependent folding and aggregation site. *J. Mol. Biol.* **334**, 477–488.
40. McColl, I. H., Blanch, E. W., Gill, A. C., Rhie, A. G. O., Ritchie, M. A., Hecht, L. *et al*. (2003). A new perspective on β-sheet structures using vibrational Raman optical activity: from poly(L-lysine) to the prion protein. *J. Am. Chem. Soc.* **125**, 10019–10026.
41. McColl, I. H., Blanch, E. W., Hecht, L. & Barron, L. D. (2004). A study of α-helix hydration in polypeptides, proteins and viruses using vibrational Raman optical activity. *J. Am. Chem. Soc.* **126**, 8181–8188.
42. Wopfner, F., Weidenhöfer, G., Schneider, R., von Brunn, A., Gilch, S., Schwarz, T. F. *et al*. (1999). Analysis of 27 mammalian and 9 avian PrPs reveals high conservation of flexible regions of the prion protein. *J. Mol. Biol.* **289**, 1163–1178.
43. van Rheede, T., Smolenaars, M. M. W., Madsen, O. & de Jong, W. W. (2003). Molecular evolution of the mammalian prion protein. *Mol. Biol. Evol.* **20**, 111–121.
44. Bamborough, P., Wille, H., Telling, G. C., Yehiely, F., Prusiner, S. B. & Cohen, F. E. (1996). Prion protein structure and scrapie replication: theoretical, spectroscopic and genetic investigations. *Cold Spring Harbor Symp. Quant. Biol.* **61**, 495–509.
45. Burns, C. S., Aronoff-Spencer, E., Legname, G., Prusiner, S. B., Antholine, W. E., Gerfen, G. J. *et al*. (2003). Copper coordination in the full-length, recombinant prion protein. *Biochemistry*, **42**, 6794–6803.
46. Warner, R. G., Hundt, C., Weiss, S. & Turnbull, J. E. (2002). Identification of the heparin sulfate binding sites in the cellular prion protein. *J. Biol. Chem.* **277**, 18421–18430.
47. Hundt, C., Peyrin, J. M., Haik, S., Gauczynski, S., Leucht, C., Rieger, R. *et al*. (2001). Identification of interaction domains of the prion protein with its 37-kDa/67-kDa laminin receptor. *EMBO J.* **20**, 5876–5886.
48. Gabus, C., Derrington, E., Leblanc, P., Chnaiderman, J., Dormont, D., Swietnicki, W. *et al*. (2001). The prion protein has RNA binding and chaperoning properties characteristic of nucleocapsid protein NCp7 of HIV-1. *J. Biol. Chem.* **276**, 19301–19309.
49. Blanch, E. W., Morozova-Roche, L. A., Cochran, D. A. E., Doig, A. J., Hecht, L. & Barron, L. D. (2000). Is polyproline II helix the killer conformation? A Raman optical activity study of the amyloidogenic prefibrillar intermediate of human lysozyme. *J. Mol. Biol.* **301**, 553–563.
50. Cooper, A. (2000). Heat capacity of hydrogen-bonded networks: an alternative view of protein folding thermodynamics. *Biophys. Chem.* **85**, 25–39.
51. Fändrich, M., Forge, V., Buder, K., Kittler, M., Dobson, C. M. & Diekmann, S. (2003). Myoglobin forms amyloid fibrils by association of unfolded polypeptide segments. *Proc. Natl Acad. Sci. USA*, **100**, 15463–15468.
52. Chiti, F., Stefani, M., Taddei, N., Ramponi, G. & Dobson, C. M. (2003). Rationalization of the effects of mutations on peptide and protein aggregation rates. *Nature*, **424**, 805–808.
53. Uversky, V. N., Gillespie, J. R. & Fink, A. L. (2000). Why are "natively unfolded" proteins unstructured under physiologic conditions? *Proteins: Struct. Funct. Genet.* **41**, 415–427.
54. Jarvet, J., Damberg, P., Danielsson, J., Johansson, I., Eriksson, L. E. G. & Gräslund, A. (2003). A left-handed 3_1 helical conformation in the Alzheimer Aβ(12–28) peptide. *FEBS Letters*, **555**, 371–374.
55. Eker, F., Griebenow, K. & Schweitzer-Stenner, R. (2004). $A\beta_{1\text{-}28}$ fragment of the amyloid peptide predominantly adopts a polyproline II conformation in acidic solution. *Biochemistry*, **43**, 6893–6898.
56. Rucker, A. L., Pager, C. T., Campbell, M. N., Qualls, J. E. & Creamer, T. P. (2003). Host-guest scale of left-handed polyproline II helix formation. *Proteins: Struct. Funct. Bioinformatics*, **53**, 68–75.
57. Chellgren, B. W. & Creamer, T. P. (2004). Short sequences of non-proline residues can adopt the polyproline II helical conformation. *Biochemistry*, **43**, 5864–5869.
58. Eker, F., Griebenow, K., Cao, X., Nafie, L. A. & Schweitzer-Stenner, R. (2004). Preferred peptide backbone conformations in the unfolded state revealed by the structure analysis of alanine-based (AXA) tripeptides in aqueous solution. *Proc. Natl Acad. Sci. USA*, **101**, 10054–10059.
59. Smith, C. K. & Regan, L. (1997). Construction and design of β-sheets. *Acc. Chem. Res.* **30**, 153–161.
60. Zahn, R., Liu, A., Lührs, T., Riek, R., von Schroetter, C., López Garcia, F. *et al*. (2000). NMR solution structure of the human prion protein. *Proc. Natl Acad. Sci. USA*, **97**, 145–150.
61. Viles, J. H., Donne, D., Kroon, G., Prusiner, S. B., Cohen, F. E., Dyson, H. J. & Wright, P. E. (2001). Local structural plasticity of the prion protein. Analysis of NMR relaxation dynamics. *Biochemistry*, **40**, 2743–2753.

62. Garcia, F. L., Zahn, R., Riek, R. & Wüthrich, K. (2000). NMR structure of the bovine prion protein. *Proc. Natl Acad. Sci. USA*, **97**, 8334–8339.
63. Kirby, L., Birkett, C. R., Rudyk, H., Gilbert, I. H. & Hope, J. (2003). *In vitro* cell free conversion of bacterial recombinant PrP to PrPres as a model for conversion. *J. Gen. Virol.* **84**, 1013–1020.
64. Whyte, S. M., Sylvester, I. D., Martin, S. R., Gill, A. C., Wopfner, F., Schatzl, H. M. *et al*. (2003). Stability and conformational properties of doppel, a prion-like protein, and its single-disulphide mutant. *Biochem. J.* **373**, 485–494.
65. Hecht, L., Barron, L. D., Blanch, E. W., Bell, A. F. & Day, L. A. (1999). Raman optical activity instrument for studies of biopolymer structure and function. *J. Raman Spectrosc.* **30**, 815–825.

Edited by P. Wright

(Received 20 July 2004; received in revised form 18 August 2004; accepted 18 August 2004)